Environmental Science & Technology

Article

Cite This: Environ. Sci. Technol. 2019, 53, 8938−8946

pubs.acs.org/est

Measure-Specific Effectiveness of Air Pollution Control on China's Atmospheric Mercury Concentration and Deposition during 2013−2017

Kaiyun Liu,[†] Qingru Wu,[†] Long Wang,[‡] Shuxiao Wang,*[,†,§] Tonghao Liu,[∥] Dian Ding,[†] Yi Tang,[†] Guoliang Li,[†] Hezhong Tian,[⊥] Lei Duan,[†,§] Xun Wang,[▽] Xuewu Fu,[▽] Xinbin Feng,[▽] and Jiming Hao[†,§]

[†]State Key Joint Laboratory of Environment Simulation and Pollution Control, School of Environment, Tsinghua University, Beijing 100084, China

[‡]School of Environment and Energy, South China University of Technology, Guangzhou 510006, China

[§]State Environmental Protection Key Laboratory of Sources and Control of Air Pollution Complex, Beijing 100084, China

[∥]China National Environmental Monitoring Centre, Beijing 100012, China

[⊥]State Key Joint Laboratory of Environmental Simulation & Pollution Control, School of Environment, Beijing Normal University, Beijing 100875, China

[▽]State Key Laboratory of Environmental Geochemistry, Institute of Geochemistry, Chinese Academy of Sciences, Guiyang 550081, China

Supporting Information

ABSTRACT: China took aggressive air pollution control measures from 2013 to 2017, leading to the mitigation of atmospheric mercury pollution as a cobenefit. This study is the first to systematically evaluate the effect of five major air pollution control measures in reducing mercury emissions, the total gaseous mercury (TGM) concentration and mercury deposition flux (FLX) for unit emissions reduction. From 2013 to 2017, China's mercury emissions decreased from 571 to 444 tons, resulting in a 0.29 ng m^{-3} decrease in the TGM concentration, on average, and in a 17 $\mu g\ m^{-2}\ yr^{-1}$ decrease in FLX. Ultralow emission renovations of coal-fired power plants are identified as the most effective emission abatement measure. As a result of this successful measure, coal-fired power plants are no longer the main mercury emitters. In 2017, the cement clinker sector became the largest emitter due to the use of less effective mercury removal measures. However, in terms of the mitigated TGM concentration and FLX levels per unit emission abatement, newly built wet flue gas desulfurization (WFGD) systems in coal-fired industrial boilers have become particularly effective in decreasing FLX levels. Therefore, to effectively reduce atmospheric mercury pollution in China, prioritizing mercury emissions control of cement clinkers and coal-fired industrial boilers is recommended.

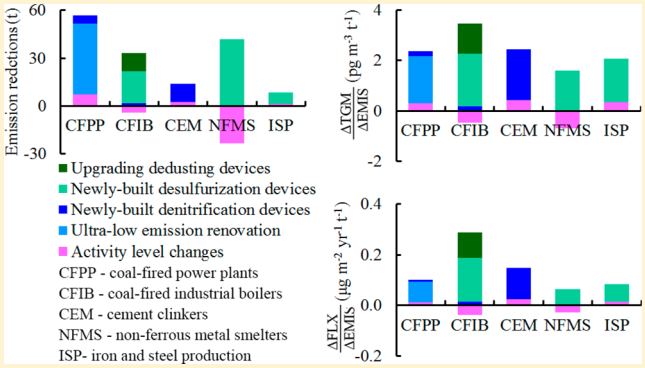

INTRODUCTION

Mercury (Hg) pollution is a major global issue due to its toxicity, long-range transport, and bioaccumulation.[1−6] To reduce global mercury emissions, the *Minamata Convention on Mercury* was signed by 128 countries on January 19, 2013 and entered into force on August 16, 2017.[7] As the most significant emitter of anthropogenic mercury, China is of central importance for global mercury emissions reduction.[5,8,9]

Zhang et al. (2015) estimated that China's anthropogenic mercury emissions continuously increased from 356 t in 2000 to 538 t in 2010, with an average annual increasing rate of 4.2%.[10] Wu et al. (2016) then expanded the emissions inventory from 1978 to 2014 using a technology-based approach at the provincial level and found the greatest contributors of mercury emissions to be coal-fired industrial boilers before 1998, zinc smelting activities from 1999−2004, coal-fired power plants from 2005−2008, and finally cement clinkers from 2009.[11] China has applied aggressive measures to control air pollution since 2013. The main emission control measures adopted include ultralow emission limits placed on coal-fired power plants, the elimination of small coal-fired boilers, and the use of clean energy for winter heating in North China, which has significantly limited levels of fine particle

Received: April 22, 2019
Revised: June 25, 2019
Accepted: June 27, 2019
Published: June 27, 2019

DOI: 10.1021/acs.est.9b02428
Environ. Sci. Technol. 2019, 53, 8938−8946

pollution.[12] These measures may also reduce atmospheric mercury emissions. Our previous studies have indicated that mercury emissions generated from coal-fired power plants decreased to 76 tons in 2015 as a result of ultralow emission renovations, and that coal-fired power plants may decrease mercury emissions by 5 $\mu g/m^3$ through ultralow emissions renovations.[13−15] While the mercury emissions reductions of various control measures have been widely studied, very few efforts have been made to evaluate related environmental quality improvements such as reductions of mercury concentrations and deposition.[9−11,16−18] Zhang et al. (2016) observed decreases (roughly 1−2% yr^{-1}) in the total gaseous mercury (TGM) concentrations from sites in North America and Europe from 1990 to 2013 due to the phasing out of mercury use in commercial products as well as cobenefits resulting from the SO_2 and NO_x emissions control of coal-fired utilities.[8] In China, a considerable decrease of the TGM concentration has also been observed at a rural station on Chongming Island resulting from the implementation of aggressive air pollution control measures since 2014.[19] However, the impacts of air pollution control measures on atmospheric mercury concentrations and deposition have not yet been quantified.

In this study, we systematically evaluated mercury emissions reductions resulting from key air pollution control measures implemented in China from 2013 to 2017 and corresponding environmental benefits resulting from the reduction of atmospheric TGM concentration and mercury deposition levels. To compare the effectiveness of these measures, we, for the first time, assess the environmental effects of unit emission reductions from each control measure. The results of this study can improve our understanding of the effectiveness of these measures, offer useful insights for the implementation of the *Minamata Convention* in China, and finally guide other countries in the design of effective mercury pollution control strategies.

MATERIALS AND METHODS

Emission control measures implemented from 2013 to 2017 mainly involved activity level changes, upgrades and building air pollution control devices (APCDs). The latter are subdivided into upgrading dedusting devices, newly built desulfurization devices, newly built denitrification devices, and ultralow emission renovations. Newly built desulfurization devices include wet flue gas desulfurization (WFGD) and dry flue gas desulfurization (DFGD) systems. Newly built denitrification devices include selective catalytic reduction (SCR) and selective noncatalytic reduction (SNCR) systems. Ultralow emission renovations mainly refer to the installation of newly built advanced electrostatic fabric filters (ESP-FFs), wet electrostatic precipitators (WESPs), and low temperature electrostatic precipitators (LTESPs). We calculated measure-specific mercury emission reductions for each sector using the China Atmospheric Mercury Emission Reduction (CAMER) model and compiled emissions data for use in the chemistry and transport model. We then ran the nested-grid GEOS-Chem model for Mainland China to estimate the impacts of anthropogenic emissions and meteorological conditions on the TGM concentration, dry deposition flux (DFLX), wet deposition flux (WFLX), and total deposition flux (FLX as the sum of DFLX and WFLX) for 2013−2017. Reductions in the TGM concentration, FLX, DFLX, and WFLX achieved by each measure were then calculated, and the corresponding measure-specific environmental impacts of unit emission reductions for an improved TGM concentration as well as FLX, DFLX, and WFLX were then evaluated.

Emission Reduction Model. The China Atmospheric Mercury Emission (CAME) model has been described in our previous work.[10,11,13] In this study, we further developed the CAMER model based on changes in activity levels (energy and material consumption, industrial products, etc.) and types and installation rates of APCDs. Mercury emission sources were divided into 29 types with 13 types of point sources and 16 types of area sources, as shown in SI Table S1. The updated CAMER model is illustrated in eqs 1 and 2.[10,16,20] Bottom-up emission variations due to activity changes for 2014−2017 relative to 2013 (RA) were calculated with eq 1 and those due to upgrades and newly built APCDs (RC) were calculated with eq 2.

$$RA = (A_t - A_{2013}) \times EF_{2013} = \sum_i \sum_j (A_{i,j,t} - A_{i,j,2013}) \times M_i \times (1 - Q_i \times W) \times \sum_m \sum_n R_m \times (1 - P_{i,m,n,2013} \times \eta_{m,n}) \quad (1)$$

$$RC = A_{2013} \times (EF_t - EF_{2013}) = \sum_i \sum_j A_{i,j,2013} \times M_i \times (1 - Q_i \times W) \times \sum_m \sum_n R_m \times (P_{i,m,n,2013} \times \eta_{m,n} - P_{i,m,n,t} \times \eta_{m,n}) \quad (2)$$

where E is mercury emissions of a certain category; A is the activity level of a given emission sector; EF is the mercury emissions factor of a given emission sector; i is the province; j is the point source; m is the type of boiler or technique used; n is the type of APCD employed; t is the calculated year; M is the mercury concentration in fuel/raw material; Q is the fraction of pretreated fuel or raw material; W is the mercury removal rate achieved by pretreatment; R is the mercury release rate of a certain type of boiler or technique; P is the proportion of a certain type of APCD; η is the mercury removal rate of a certain type of APCD; RA is the degree of mercury emission reduction due to activity changes; and RC is the degree of mercury emission reduction attributable to APCD upgrading and rebuilding.

Based on the dominance of mercury emission sources and the availability of essential data, all categories were ranked into three tiers. Methods and key parameters used for the three tiers are detailed in SI Sections 1−6, Tables S1−S7, and Figures S1−S4. Activity levels, APCD types and provincial installation rates are summarized in Table S1.[21−25] Databases of emission factors (SI Table S2), provincial mercury content in fuels/raw materials (SI Tables S3−S4), mercury speciation in exhausted flue gas (SI Table S5), and APCD removal efficiencies (SI Tables S6−S7) are elaborated based on our previous studies.[10,11,13,26−30]

A Monte Carlo simulation was used to analyze uncertainty in mercury emissions based on the probability distribution of key parameters. A normal distribution with a coefficient of variation (CV or the standard deviation divided by the mean) of 5% was assumed for activity levels. Mercury content levels of fuels/raw materials fit a log-normal distribution curve, as shown in SI Tables S2−S3.[10,11,13,30,31] The distribution characteristics of APC' removal efficiencies are shown in SI Tables S5 and S6.[10,11,13,30] We ran the simulations 10 000 times and obtained results in the form of a statistical distribution. We set (P50−P10)/P50 and (P90−P50)/P50 values as the lower and upper limit of the uncertainty range

DOI: 10.1021/acs.est.9b02428
Environ. Sci. Technol. 2019, 53, 8938−8946

Table 1. Scenario Descriptions

scenarios	meteorology	anthropogenic mercury emissions	cases	notes
BASE	2013−2017	anthropogenic emissions for 2013−2017	5	baseline simulations
METE	2014−2017	anthropogenic emissions for 2013	4	to quantify impacts of variations in meteorology
CTRL	2013	2013 anthropogenic emissions after individually deducting emission reductions from 5 control measures for 5 major sources	13	to quantify impacts of each measure

with a confidence level of 80%. The overall degree of uncertainty in China's anthropogenic mercury emissions was estimated to range from −20% to 23%. Further information on uncertainty ranges of the 29 types of mercury emission sources are illustrated in SI Figure S5.

GEOS-Chem Model. The GEOS-Chem model is a global 3-D model of atmospheric chemistry and transport driven by assimilated meteorological data from the Goddard Earth Observing System (GEOS) of the NASA Global Modeling and Data Assimilation Office (GMAO). The nested-grid mercury simulation approach was developed by Zhang et al. (2012) for the North American domain.[32] Wang et al. (2014) adopted it for TGM nested-grid simulations of East Asian domain with a spatial resolution of 0.5° × 0.625°.[33] In this study, the nested-grid GEOS-Chem model (version 11−01; http://geos-chem.org) is applied to Mainland China (15°N−55°N, 70°E−140°E) using 161 × 225 horizontal grids. The spatial resolution is set to 0.25° × 0.3125° (roughly 20 × 25 km for China) with 47 vertical layers from the surface to roughly 80 km in altitude. The global GEOS-Chem model with a resolution of 2° × 2.5° was ran for 2010−2017 to provide initial and boundary conditions. The updated mercury concentration for surface soil (0−20 cm) in China given in Wang et al. (2016) is quoted by the nested-grid GEOS-Chem model for the Chinese domain (GEOS-Chem-CH).[34] Simulated mercury emissions from surface soil are shown in SI Figure S6.

As input for the GEOS-Chem model, gridded emission inventories with a spatial resolution of 0.25° × 0.3125° for gaseous elemental mercury (GEM), gaseous oxidized mercury (GOM), and particulate-bound mercury (PBM) were obtained, as shown in SI Figure S7. Emissions of roughly 8000 point sources were gridded according to their locations, longitudes, and latitudes, accounting for more than 70% of China's mercury emissions. Emissions of area sources were gridded according to spatial distributions of population, GDP, and road networks.[35] It is worth noting that, in general, China's anthropogenic mercury emissions were increasing from 1978 to 2012 and basically peaked in 2013 (SI Figure S8).[11] Therefore, we apply the 2013−2017 period as the simulated time scale.

To evaluate the model's performance, we compared simulations of the surface TGM concentration and wet and dry deposition flux with observations from the published literature for remote stations (SI Tables S8−S9).[19,36−48] The time period of the simulation is consistent with observations for each station. As shown in SI Table S8, the mean TGM concentration derived from observations made at land stations is 2.12 ± 0.84 ng/m^3, whereas that of the simulations is 2.02 ± 0.39 ng/m^3. As illustrated in SI Figure S9, the observed annual and seasonal mean TGM concentrations are successfully reproduced by the GEOS-Chem-CH model with the input of our highly resolved mercury emission inventory. For wet and dry deposition flux, the model also corresponds well with observations shown in SI Figure S10 within a factor of 1.5.

Simulation Scenarios. In this study, the receptor domain for analysis was Mainland China, which includes 31 Chinese provinces, autonomous regions, and municipalities with the exception of Hong Kong, Macao, and Taiwan. As shown in Table 1, four scenarios were utilized to simulate the TGM concentration, DFLX, WFLX, and FLX. BASE scenarios were simulated with the input of anthropogenic mercury emissions and meteorology conditions for the same year of the 2013−2017 period. The difference found between BASE 2014−2017 scenarios and the BASE 2013 scenario reflects the total change in the TGM concentration, DFLX, WFLX, and FLX. The METE scenarios were simulated with 2013 emissions and from varying meteorological conditions for 2014−2017. The impact of meteorological conditions was quantified as the difference between 2014 and 2017 METE scenarios and the 2013 BASE scenario. The effect of total anthropogenic mercury emissions reduction was quantified as the difference between METE and BASE scenarios for the same year, which was calculated as equal to the corresponding total change without the impact of meteorological conditions.

Emission reductions shaped by five measures of five major sources were individually subtracted to generate input data for CTRL scenarios. Measure-specific improvements of the TGM concentration and mercury deposition were derived from BASE 2013 and CTRL scenarios. $\Delta EMIS_{c,j}$ represents mercury emission reductions over Mainland China due to emission control measure c being applied to major source j from 2013 to 2017. $\Delta TGM_{c,j}$, $\Delta DFLX_{c,j}$, $\Delta WFLX_{c,j}$, and $\Delta FLX_{c,j}$ are the decreases in the TGM concentration, DFLX, WFLX and FLX, respectively. Therefore, the measure-specific benefits of unit emission reduction for he mitigated TGM concentration $(\frac{\Delta TGM_{c,j}}{\Delta EMIS_{c,j}})$ and DFLX $(\frac{\Delta DFLX_{c,j}}{\Delta EMIS_{c,j}})$, WFLX $(\frac{\Delta WFLX_{c,j}}{\Delta EMIS_{c,j}})$ and FLX $(\frac{\Delta FLX_{c,j}}{\Delta EMIS_{c,j}})$ could be calculated.

RESULTS AND DISCUSSION

Measure-Specific Emission Abatements for 2013−2017. Total atmospheric mercury emissions in China continuously decreased from 571 tons in 2013 to 444 tons in 2017, reflecting a 22% reduction. Coal-fired power plants, coal-fired industrial boilers, nonferrous metal smelters, cement clinkers, and iron and steel production accounted for 45%, 23%, 15%, 11%, and 6% of the total reduction, respectively.

For coal-fired power plants, APCDs for ultralow emissions were increasingly retrofitted or built from 2013 to 2017 to achieve stringent PM emission limits (GB13223−2011).[49] As illustrated in SI Figure S3, the proportion of APCDs for ultralow emissions increased from 0% in 2013 to 72% in 2017, which resulted in 45 tons of mercury emission reductions (SI Table S10). In addition, 147 Mt of feed coal was saved as a result of the "Substitution of Smaller Units with Large Units" policy, which reduced mercury emissions by 7 tons. In addition, the popularity of SCR reduced 5 tons of mercury

DOI: 10.1021/acs.est.9b02428
Environ. Sci. Technol. 2019, 53, 8938−8946

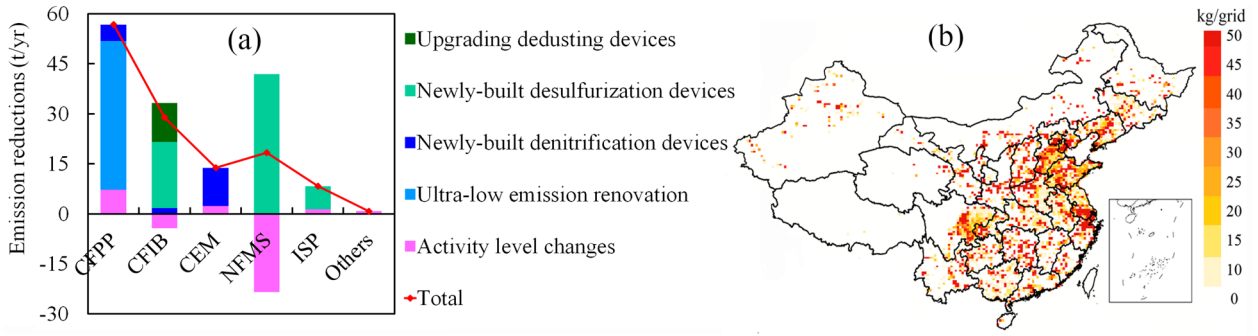

Figure 1. Measure-specific benefits of the major sources of mercury emission reduction for 2013−2017 (a) and the distribution of total mercury emission reductions (b); CFPP denotes coal-fired power plants; CFIB denotes coal-fired industrial boilers, including all coal consumption sectors except for CFPP operation and residential coal combustion; NFMS denotes nonferrous metal smelters, including Zn, Pb, and Cu smelters; CEM denotes cement clinkers; ISP denotes iron and steel production.

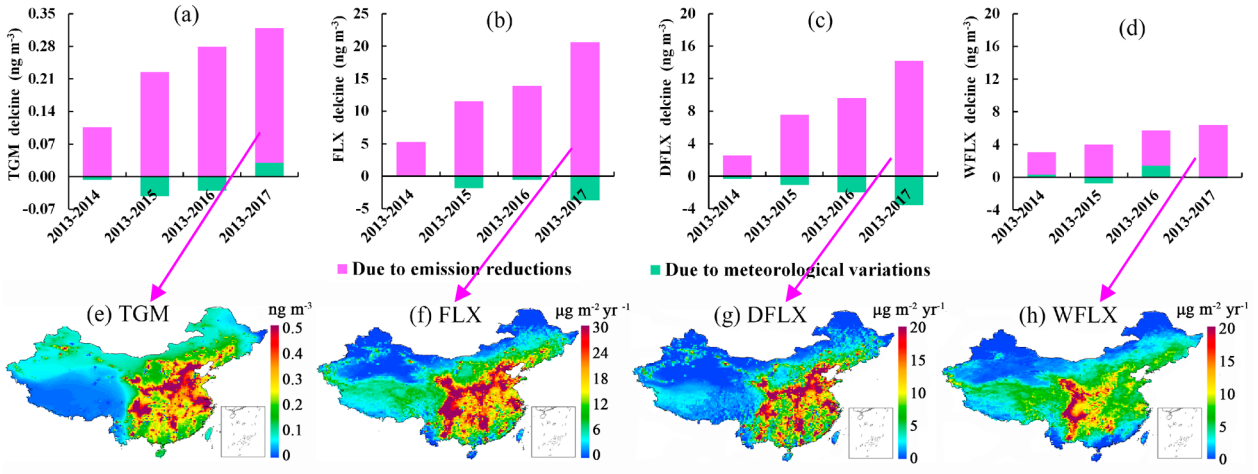

Figure 2. Annual changes in the TGM concentration, FLX, DFLX, and WFLX from 2014 to 2017 relative to 2013 levels due to anthropogenic mercury emission reductions and meteorological variations (a)−(d); The distribution of the annual decreased TGM concentration, FLX, DFLX, and WFLX for 2013 to 2017 due to anthropogenic mercury emission reductions alone (e)−(h).

emissions. Consequently, in China, 57 tons of mercury emissions were cut through these measures. As shown in SI Table S10, coal-fired power plants dominated emission reductions in most of the regions except in Central China.

For coal-fired industrial boilers, the WFGD application rate increased from 5% in 2013 to 45% in 2017, cutting 20 tons of mercury emissions. Cyclone (CYC) and wet scrubber (WET) instruments have also been gradually replaced with integrated dust removal devices (IDRDs), electrostatic precipitators (ESPs), and fabric filters (FFs) since 2013, as shown in SI Figure S4. By the end of 2017, 45% of coal-fired industrial boilers installed IDRDs and 55% were equipped with ESPs/FFs, cutting 12 tons of mercury emissions. However, higher levels of coal consumption in 2017 produced 4 tons of additional mercury emissions. It is worth noting that the shift from coal to gas and the closure of small boilers achieved initial success in East China and especially in the Beijing-Tianjin-Hebei region, as shown in SI Table S10.

As for cement clinkers, the SCR/SNCR installation rate was increased from 30% in 2013 to 90% in 2017, reducing mercury emissions by 11 tons. Reductions to cement production from 2013 to 2017 cut 2 tons of mercury emissions. Mercury emissions generated through iron and steel production decreased by 7 tons, owing to newly built WFGD systems, whereas levels were decreased by 1 ton due to lower activity levels in 2017. For nonferrous metal smelters, mercury emissions decreased by 42 tons through the adoption of newly built FGD (WFGD and DFGD) systems, whereas 23 more tons were emitted due to higher production in 2017. In Central China, 53% of emission reductions were a result of nonferrous metal smelter use. SI Table S10 presents major sources of emission reductions due to the five measures for different regions from 2013 to 2017.

In general, with respect to measure-specific emission abatements, the adoption of newly built APCDs to ensure ultralow emissions from coal-fired power plants was the most effective measure followed by the use of newly built FGDs in nonferrous metal smelters and of newly built WFGDs in coal-fired industrial boilers. Figure 1(b) shows the distribution of mercury emission reductions for 2013−2017. East China and Southwest China have been remarkable in terms of mitigating anthropogenic mercury emissions and especially in Beijing-Tianjin-Hebei (BTH), the Yangtze River Delta (YRD), and Sichuan-Chongqing (SC).

Improved Atmospheric Mercury Pollution Levels for 2013−2017. Along with the 127 tons of anthropogenic mercury emission reductions, the national annual TGM concentration, FLX, DFLX, and WFLX were found to decrease from 2.67 ng m^{-3}, 85 $\mu g\ m^{-2}\ yr^{-1}$, 55 $\mu g\ m^{-2}\ yr^{-1}$, and 30 $\mu g\ m^{-2}\ yr^{-1}$ in 2013 to 2.35 ng m^{-3}, 68 $\mu g\ m^{-2}\ yr^{-1}$, 44 $\mu g\ m^{-2}$

DOI: 10.1021/acs.est.9b02428
Environ. Sci. Technol. 2019, 53, 8938−8946

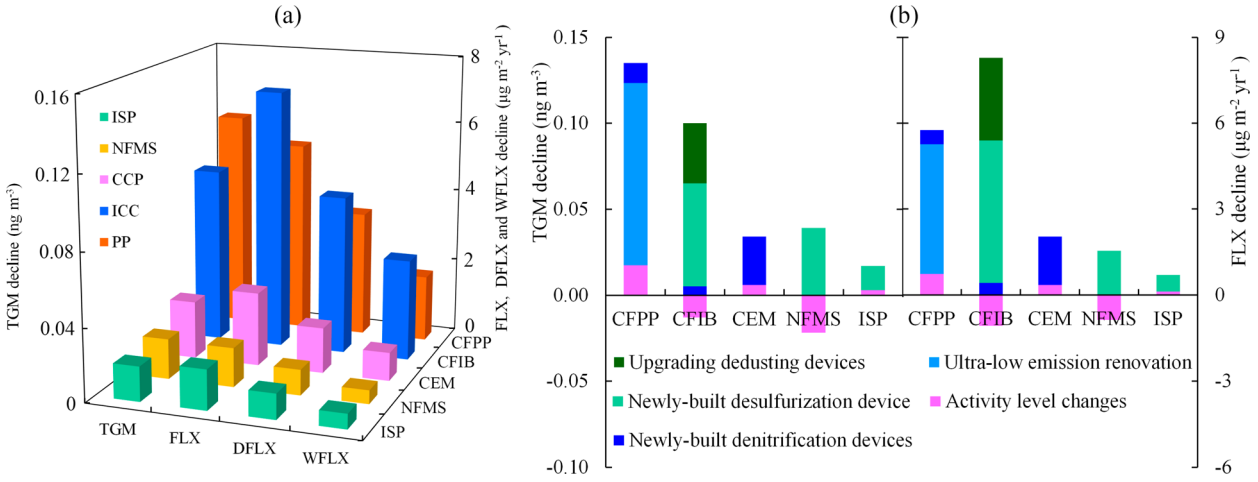

Figure 3. Major source contributions to the decrease in the TGM concentration, FLX, DFLX, and WFLX (a); measure-specific benefits of reductions in the TGM concentration and FLX (b).

yr^{-1}, and 24 $\mu g\ m^{-2}\ yr^{-1}$ in 2017, respectively. Relative to 2013 levels, FLX, DFLX, and WFLX in 2017 decreased by roughly 20%, which is much higher than the observed decrease in the TGM concentration (12%). These results show that mercury deposition is more heavily influenced by local anthropogenic mercury emissions than by the TGM concentration.

Figure 2 (a)−(d) compares annual changes in the TGM concentration, FLX, DFLX, and WFLX for 2014−2017 relative to 2013 levels due to anthropogenic mercury emission reductions and interannual meteorological variations. Meteorologically driven variabilities of TGM concentration were estimated at −0.04−0.03 ng m^{-3}, which are much lower than the contributions of 0.11−0.29 ng m^{-3} observed for anthropogenic emission abatements. Meteorological variations impacted −4−2 $\mu g\ m^{-2}\ yr^{-1}$ of FLX, −3.5−0.5 $\mu g\ m^{-2}\ yr^{-1}$ of DFLX and −0.5−1.5 $\mu g\ m^{-2}\ yr^{-1}$ of WFLX, which are also much lower than variabilities observed for FLX (5−21 $\mu g\ m^{-2}\ yr^{-1}$), DFLX (2−14 $\mu g\ m^{-2}\ yr^{-1}$), and WFLX (3−7 $\mu g\ m^{-2}\ yr^{-1}$) driven by anthropogenic emission abatements. These results indicate that abatements of the TGM concentration, FLX, DFLX, and WFLX from 2013 to 2017 were dominated by anthropogenic mercury emission reductions rather than by interannual meteorological variations.

Figure 2 (e)−(h) shows the spatial distribution of the mitigated TGM concentration, FLX, DFLX, and WFLX for China in 2017 relative to 2013 levels. The TGM concentration decreases in East, Central, and Southwest China. The TGM concentration decreased by as much as 0.5 ng m^{-3} in BTH, the YRD and SC, consistent with the distribution of anthropogenic mercury emission reductions, as shown in Figure 1(b). As the TGM concentration is a major DFLX-related factor, the distribution of the DFLX decrease is similar to the distribution of the TGM decrease. However, a major distinction in the distribution of WFLX reductions can be observed. High local emission reductions combined with high levels of precipitation produce in the highest levels of WFLX decrease in Southwest China. Particularly, in parts of SC, the WFLX levels decreased by over 20 $\mu g\ m^{-2}\ yr^{-1}$. Consequently, FLX mitigation was mainly concentrated in East, Central, and Southwest China.

Measure-Specific Improvements of Atmospheric Mercury Pollution. A comparison of the major source contributions to the decrease in the TGM concentration, FLX, DFLX, and WFLX, as shown in Figure 3(a), to the emission reductions shown in Figure 1(a) in 2017 relative to those in 2013 reveals that coal-fired power plants were the top contributors regardless of the TGM concentration decreases or emission reductions followed by coal-fired industrial boilers. Both sectors together showed a 0.22 ng m^{-3} reduction of the TGM concentration, accounting for 76% of TGM concentration abatements. However, for FLX, DFLX, and WFLX decreases, coal-fired industrial boilers were the top contributors, followed by coal-fired power plants. These decreases mainly occurred because the emission reductions caused by coal-fired industrial boilers had a broader distribution than those caused by coal-fired power plants. Both sectors together accounted for roughly 79% of FLX, DFLX, and WFLX reductions.

From the simulated scenarios, we further estimated measure-specific contributions to the decreases in the TGM concentration and FLX, as shown in Figure 3(b). Ultralow emissions renovations of coal-fired power plants were the most effective at mitigating the TGM concentration, decreasing the TGM concentration by as much as 0.1 ng m^{-3}. This measure was also the most effective for emission abatements. However, newly built WFGD systems in coal-fired industrial boilers contributed the most to FLX reductions (5.0 $\mu g\ m^{-2}\ yr^{-1}$) followed by ultralow emission renovations of coal-fired power plants (4.5 $\mu g\ m^{-2}\ yr^{-1}$).

From a comparison of mercury mass-balance levels observed under the BASE and CTRL scenarios (SI Figure S11), we found that roughly 65 tons of mercury deposition in Mainland China and roughly 52 tons of net mercury outflows were cut through anthropogenic mercury emission reductions. As shown in SI Figure S12, the measure of newly built WFGD systems in coal-fired industrial boilers contributed the most to mercury deposition reduction in Mainland China (20 tons), whereas ultralow emission renovations of coal-fired power plants reduced net mercury outflows by as must as 19 tons.

In addition, the most effective measure varies by region. As shown in SI Figure S13, in Central China, the most effective measure for improving the TGM concentration, FLX, DFLX, and WFLX was found to be newly built FGD devices used in nonferrous metal smelters. However, in North China, newly built WFGD devices used in coal-fired industrial boilers achieved the greatest improvements of the TGM concentration, FLX, DFLX, and WFLX. For other regions, ultralow

DOI: 10.1021/acs.est.9b02428
Environ. Sci. Technol. 2019, 53, 8938−8946

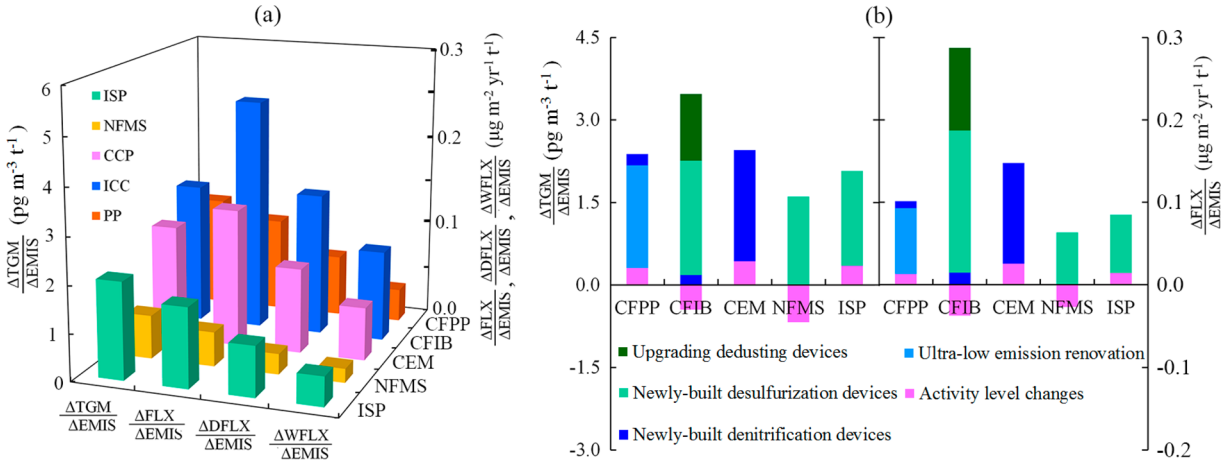

Figure 4. Environmental impacts of unit emission reductions on the TGM concentration, FLX, DFLX, and WFLX (a); measure-specific benefits of unit emission reductions on the TGM concentration and FLX (b).

renovations of coal-fired power plants spurred the greatest decrease in the TGM concentration, whereas newly built WFGD devices led to the largest decreases in FLX, DFLX, and WFLX.

Measure-Specific Benefits of Unit Emissions Reductions. We also calculated the measure-specific benefits of unit emission abatement for the mitigated TGM concentration, FLX, DFLX, and WFLX for 2017 relative to 2013 (Figure 4). Higher values of ΔTGM/ΔEMIS, ΔFLX/ΔEMIS, ΔDFLX/ΔEMIS, and ΔWFLX/ΔEMIS denote more significant decreases in the TGM concentration, FLX, DFLX, and WFLX resulting from unit emission reductions. As illustrated in Figure 4(a), for the decrease in the TGM concentration, the benefits of unit emission reductions resulting from coal-fired industrial boilers (0.003 ng m^{-3} t^{-1}) were found to be stronger than those of cement clinkers (0.0025 ng m^{-3} t^{-1}) and coal-fired power plants (0.0024 ng m^{-3} t^{-1}). For FLX, DFLX, and WFLX, the environmental impacts of unit emission reductions resulting from coal-fired industrial boilers (0.25 μg m^{-2} yr^{-1} t^{-1}, 0.15 μg m^{-2} yr^{-1} t^{-1}, and 0.1 μg m^{-2} yr^{-1} t^{-1}) were also the highest at the national level. As shown in Figure 4(b), for TGM mitigation from 2013 to 2017, the environmental benefit of newly built WFGD devices used in coal-fired industrial boilers was slightly stronger than that resulting from ultralow emission renovations of coal-fired power plants. For FLX mitigation, the environmental benefits of newly built WFGD device use in coal-fired industrial boilers were more prominent. Differences in measure-specific benefits observed are mainly attributed to fact that emission sources varied in geographical distribution (SI Figure S1) and mercury speciation in exhausted flue gas (SI Table S5).

Because the precursor of TGM and FLX was the emitted mercury from various sources, Brute-Force Method (BBM) was performed to estimate measure-specific and major source contributions to ΔTGM and ΔFLX.[8,50−52] SI Figure S14 compared the additive major source contributions to ΔTGM and ΔFLX with the baseline levels. The additive ΔTGM was 0.27 ng m^{-3} and the baseline ΔTGM was 0.29 ng m^{-3}. The additive ΔFLX was 16 μg m^{-2} yr^{-1} and the baseline ΔFLX was 17 μg m^{-2} yr^{-1}. Overall, the relative deviations of brute-force method for ΔTGM and ΔFLX were less than 10%. If multiple sensitive parameters (such as precursor emissions, dry deposition parametrization, oxidizing species ambient concentrations, etc.) for TGM concentration and FLX are taken into account, BBM may not capture the nonlinear effects. To address this issue, CMAQ-Hg model with the Decoupled Direct Method (DDM) may be needed.

From a comparison of Figures 1, 3, and 4, two research findings are identified. First, unit emission reductions resulting from sources characterized by broader distributions can achieve stronger environmental benefits. For example, coal-fired power plants spurred the most significant emission reductions and significant decreases in the TGM concentration, FLX, DFLX, and WFLX, but the corresponding environmental impacts of unit emission reductions were much less significant than those of coal-fired industrial boilers, especially in terms of FLX, DFLX, and WFLX. These result were mainly because coal-fired industrial boilers are scattered across the country, whereas coal-fired power plants are concentrated within or close to coastal provinces and coal-electricity bases. Ultralow emission renovations of coal-fired power plants were the most effective at reducing emissions and mitigating TGM levels, but their environmental impacts on unit emission reductions were less significant than those of newly built WFGD devices in coal-fired industrial boilers. The limited environmental impacts of unit emission reductions of nonferrous metal smelters tend to highlight this phenomenon, as nonferrous metal smelters are mainly located in Central China.

Second, we found that unit emission reductions from sources characterized by a higher proportion of GOM in exhausted flue gas can better mitigate mercury concentrations and deposition.[8] WFGD can wash out most of GOM in exhausted flue gas.[27] SCR catalysts can promote the oxidation of GEM to GOM, resulting in more GOM being removed by WFGD gypsum.[13,53] For cement clinkers, the installation rate of SCR/SNCR increased from 30% in 2013 to 90% in 2017, but little WFGD was applied. For coal-fired power plants, the installation rate of SCR/SNCR increased from 45% in 2013 to 92% in 2017, whereas WFGD was widely applied from 2013 to 2017. Consequently, the proportion of GOM in cement clinker flue gas was as high as roughly 51% in dry-process precalciner systems with dust recycling, whereas the proportion of GOM reached 20∼30% in the flue gas of coal-fired power plants.[27,54] Almost all of the GOM emitted from cement clinkers tended to be deposited locally, whereas GEM tended toward long-range transport.[8,55,56] Moreover, most coal-fired power plants are located in the coastal provinces, facilitating the cross-

DOI: 10.1021/acs.est.9b02428
Environ. Sci. Technol. 2019, 53, 8938−8946

border transport of GEM. Therefore, the environmental impacts of unit emission reductions resulting from cement clinkers were stronger than those of coal-fired power plants and especially in terms of FLX, DFLX, and WFLX. Similarly, newly built SCR/SNCR devices used in cement clinkers can achieve stronger environmental benefits than ultralow emission renovations of coal-fired power plants.

Policy Implications. As the largest anthropogenic mercury emitter and as one of the most polluted countries in the world, China has been attempting to address this issue in recent years.[10,11,13,30] From 2013 to 2017, China reduced anthropogenic mercury emissions by 127 tons through the application of five measures of five major source categories, mitigating 12% of the TGM concentration and 20% of mercury deposition. However, in 2017, China's anthropogenic mercury emissions, mercury concentrations and deposition levels were still much higher than those in North America and Europe.[5,57] Therefore, China is under considerable domestic and international pressure to develop a national implementation plan for the *Minamata Convention* as soon as possible.

Regarding mercury emissions, as shown in SI Table S12, coal-fired power plants are no longer the main emitters due to the successful implementation of ultralow emission renovations. By the end of 2017, nearly 72% of all coal-fired power plants were equipped with APCDs for ultralow emissions, resulting in limiting the potential for further mercury emission reductions. In 2017, the cement clinker sector was the largest mercury emitter (SI Figure S15) and contributor to mercury concentrations and deposition (SI Table S12). Although SCR/SNCR and ESP/FF have been widely applied in Chinese cement clinkers, dust recycling through the precalciner process results in low mercury removal efficiencies of APCDs.[54] As a result, minor emission reductions (Figure 1) and limited improvements in mercury concentrations and deposition levels (Figure 3) were achieved from 2013 to 2017. Consequently, it is urgently necessary to limit the buildup of mercury levels in kiln dust using specific mercury removal (SMR) measures to effectively reduce the mercury emissions of cement clinkers. However, in terms of environmental benefits (reductions of TGM and FLX in this study) of unit emission reductions, the coal-fired industrial boiler sector is prominent, especially for FLX mitigation. The use of newly built WFGD devices in coal-fired industrial boilers was also identified to be the most effective measure (Figure 4). By the end of 2017, only 45% of coal-fired industrial boilers were equipped with WFGD devices. Therefore, we recommend promoting the use of newly built WFGD systems in all coal-fired industrial boilers. In sum, we recommend prioritizing cement clinker emission control by SMR and coal-fired industrial boiler emissions control by WFGD for *Convention* adherence.

It is noteworthy that with increasing mercury emission reductions from China's anthropogenic sources, coordinated emission reductions at the global scale and especially from neighboring countries' anthropogenic sources become more and more important for the mitigation of local atmospheric mercury pollution. The results of this study may be used by other developing countries in adhering to the *Minamata Convention on Mercury*.

■ ASSOCIATED CONTENT

Supporting Information

The Supporting Information is available free of charge on the ACS Publications website at DOI: 10.1021/acs.est.9b02428.

Methods and parameters for mercury emission reduction (sections 1−7, Tables S1−S7, Figures S1−S5); Descriptions of the model evaluation and simulation (sections 8−10, Tables S6−S10, Figures S8−S10); Result analysis (sections 11−13, Tables S11−S13, Figures S11−S15) (PDF)

■ AUTHOR INFORMATION

Corresponding Author

*Phone: +86 10 62771466; fax: +86 10 62773597; e-mail: shxwang@tsinghua.edu.cn.

ORCID

Qingru Wu: 0000-0003-3381-4767
Shuxiao Wang: 0000-0001-9727-1963
Hezhong Tian: 0000-0002-3638-8495
Lei Duan: 0000-0001-9965-4618
Xun Wang: 0000-0002-7407-8965
Xuewu Fu: 0000-0002-5174-7150
Xinbin Feng: 0000-0002-7462-8998

Notes

The authors declare no competing financial interest.

■ ACKNOWLEDGMENTS

This work was funded through the Pan-Third Pole Environment Study for a Green Silk Road (Pan-TPE) (XDA20040502) and the National Research Program for Key Issue in Air Pollution Control (DQGG0101).

■ REFERENCES

(1) Schroeder, W. H.; Munthe, J. Atmospheric mercury - An overview. *Atmos. Environ.* **1998**, *32* (5), 809−815.

(2) Zahir, F.; Rizwi, S. J.; Haq, S. K.; Khan, R. H. Low dose mercury toxicity and human health. *Environ. Toxicol. Pharmacol.* **2005**, *20* (2), 351−360.

(3) Wolfe, M. F.; Schwarzbach, S.; Sulaiman, R. A. Effects of mercury on wildlife: a comprehensive review. *Environ. Toxicol. Chem.* **1998**, *17* (2), 146−160.

(4) Fu, X. W.; Feng, X. B.; Sommar, J.; Wang, S. F. A review of studies on atmospheric mercury in China. *Sci. Total Environ.* **2012**, *421*−*422*, 73.

(5) Horowitz, H. M.; Jacob, D. J.; Zhang, Y.; Dibble, T. S.; Slemr, F.; Amos, H. M.; Schmidt, J. A.; Corbitt, E. S.; Marais, E. A.; Sunderland, E. M. A new mechanism for atmospheric mercury redox chemistry: implications for the global mercury budget. *Atmos. Chem. Phys.* **2017**, *17* (10), 6353−6371.

(6) M, D.; A, H. A.; C, L. H.; M, K. R.; M, M.; S, M.; S, A. H.; Risks, P. o. H.; Methylmercury, T. E. o.. Methylmercury exposure and health effects in humans: a worldwide concern. *Ambio* **2007**, *36* (1), 3−11.

(7) United Nations Environment Programme (UNEP). *Minamata Convention on Mercury*; UNEP: Geneva, Switzerland, 2013.

(8) Zhang, Y.; Jacob, D. J.; Horowitz, H. M.; Chen, L.; Amos, H. M.; Krabbenhoft, D. P.; Slemr, F.; St Louis, V. L.; Sunderland, E. M. Observed decrease in atmospheric mercury explained by global decline in anthropogenic emissions. *Proc. Natl. Acad. Sci. U. S. A.* **2016**, *113* (3), 526−531.

(9) United Nations Environment Programme (UNEP). *Global Mercury Assessment 2013: Sources, Emissions, Releases and Environmental Transport*; UNEP: Geneva, Switzerland, 2013.

(10) Zhang, L.; Wang, S.; Wang, L.; Wu, Y.; Duan, L.; Wu, Q.; Wang, F.; Yang, M.; Yang, H.; Hao, J.; Liu, X. Updated emission inventories for speciated atmospheric mercury from anthropogenic sources in China. *Environ. Sci. Technol.* **2015**, *49* (5), 3185−3194.

(11) Wu, Q.; Wang, S.; Li, G.; Liang, S.; Lin, C.-J.; Wang, Y.; Cai, S.; Liu, K.; Hao, J. Temporal trend and spatial distribution of speciated

atmospheric mercury emissions in China during 1978−2014. *Environ. Sci. Technol.* **2016**, *50* (24), 13428−13435.
(12) Clean Air Alliance of China (CAAC). *China's Clean Air Action Plan*; CAAC: Beijing, China, 2013.
(13) Liu, K.; Wang, S.; Wu, Q.; Wang, L.; Ma, Q.; Zhang, L.; Li, G.; Tian, H.; Duan, L.; Hao, J. A highly-resolved mercury emission inventory of Chinese coal-fired power plants. *Environ. Sci. Technol.* **2018**, *52* (4), 2400−2408.
(14) Wu, Q.; Li, G.; Wang, S.; Liu, K.; Hao, J. Mitigation Options of Atmospheric Hg Emissions in China. *Environ. Sci. Technol.* **2018**, *52* (21), 12368−12375.
(15) Wu, Q.; Wang, S.; Liu, K.; Li, G.; Hao, J. Emission-limit-oriented strategy to control atmospheric mercury emissions in coal-fired power plants toward the implementation of the minamata convention. *Environ. Sci. Technol.* **2018**, *52* (19), 11087−11093.
(16) Streets, D. G.; Hao, J.; Wu, Y.; Jiang, J.; Chan, M.; Tian, H.; Feng, X. Anthropogenic mercury emissions in China. *Atmos. Environ.* **2005**, *40* (39), 7789−7806.
(17) Pacyna, E. G.; Pacyna, J. M.; Sundseth, K.; Munthe, J.; Kindbom, K.; Wilson, S.; Steenhuisen, F.; Maxson, P. Global emission of mercury to the atmosphere from anthropogenic sources in 2005 and projections to 2020. *Atmos. Environ.* **2010**, *44* (20), 2487−2499.
(18) Tian, H.; Liu, K.; Hao, J.; Wang, Y.; Gao, J.; Qiu, P.; Zhu, C. Nitrogen oxides emissions from thermal power plants in china: current status and future predictions. *Environ. Sci. Technol.* **2013**, *47* (19), 11350−11357.
(19) Tang, Y.; Wang, S.; Wu, Q.; Liu, K.; Wang, L.; Li, S.; Gao, W.; Zhang, L.; Zheng, H.; Li, Z. Recent decrease trend of atmospheric mercury concentrations in East China: the influence of anthropogenic emissions. *Atmos. Chem. Phys.* **2018**, *18* (11), 8279−8291.
(20) Muntean, M.; Janssens-Maenhout, G.; Song, S.; Selin, N. E.; Olivier, J. G. J.; Guizzardi, D.; Maas, R.; Dentener, F. Trend analysis from 1970 to 2008 and model evaluation of EDGARv4 global gridded anthropogenic mercury emissions. *Sci. Total Environ.* **2014**, *494*−*495*, 337−350.
(21) China Electricity Council *Chinese Statistics of Electric Power Industry*; China Power Press: Beijing, China, 2013−2017.
(22) China National Environmental Monitoring Centre (CNEMC). *Chinese Environmental Statistics (Collected from Provincial Environmental Protection Bureaus)*; CNEMC: Beijing, China, 2013−2017.
(23) Ministry of Ecology and Environment of the People's Republic of China (MEE). Management system of pollutant mission permit (http://permit.mee.gov.cn/).
(24) National Energy Statistical Agency of China (NESA). *China Energy Statistical Yearbook*. NESA: Beijing, China, 2014−2017.
(25) National Bureau of Statistics of China (NBSC). *China Statistical Yearbook*. NBSC: Beijing, China, 2014−2018.
(26) Tian, H.; Liu, K.; Zhou, J.; Lu, L.; Hao, J.; Qiu, P.; Gao, J.; Zhu, C.; Wang, K.; Hua, S. Atmospheric emission inventory of hazardous trace elements from China's coal-fired power plants–temporal trends and spatial variation characteristics. *Environ. Sci. Technol.* **2014**, *48* (6), 3575−3582.
(27) Zhang, L.; Wang, S.; Meng, Y.; Hao, J. Influence of mercury and chlorine content of coal on mercury emissions from coal-fired power plants in china. *Environ. Sci. Technol.* **2012**, *46* (11), 6385−6392.
(28) Wu, Q. R.; Wang, S. X.; Zhang, L.; Song, J. X.; Yang, H.; Meng, Y. Update of mercury emissions from China's primary zinc, lead and copper smelters, 2000−2010. *Atmos. Chem. Phys.* **2012**, *12* (22), 11153−11163.
(29) Yang, H. *Study on Atmospheric Mercury Emission and Control Strategies from Cement Production in China*, M.S. thesis, Tsinghua University: Beijing, China, 2014.
(30) Wu, Q.; Gao, W.; Wang, S.; Hao, J. Updated atmospheric speciated mercury emissions from iron and steel production in China during 2000−2015. *Atmos. Chem. Phys.* **2017**, *17* (17), 10423−10433.
(31) Tian, H.; Liu, K.; Zhou, J.; Lu, L.; Hao, J.; Qiu, P.; Gao, J.; Zhu, C.; Wang, K.; Hua, S. Atmospheric Emission Inventory of Hazardous Trace Elements from China's Coal-Fired Power Plants—Temporal Trends and Spatial Variation Characteristics. *Environ. Sci. Technol.* **2014**, *48* (6), 3575−3582.
(32) Zhang, Y.; Jaeglé, L.; van Donkelaar, A.; Martin, R. V.; Holmes, C. D.; Amos, H. M.; Wang, Q.; Talbot, R.; Artz, R.; Brooks, S.; Luke, W.; Holsen, T. M.; Felton, D.; Miller, E. K.; Perry, K. D.; Schmeltz, D.; Steffen, A.; Tordon, R.; Weiss-Penzias, P.; Zsolway, R. Nested-grid simulation of mercury over North America. *Atmos. Chem. Phys.* **2012**, *12* (14), 6095−6111.
(33) Wang, L.; Wang, S. X.; Zhang, L.; Wang, Y. X.; Zhang, Y. X.; Nielsen, C.; McElroy, M. B.; Hao, J. M. Source apportionment of atmospheric mercury pollution in China using the GEOS-Chem model. *Environ. Pollut.* **2014**, *190*, 166−175.
(34) Wang, X.; Lin, C.-J.; Yuan, W.; Sommar, J.; Zhu, W.; Feng, X. Emission-dominated gas exchange of elemental mercury vapor over natural surfaces in China. *Atmos. Chem. Phys.* **2016**, *16* (17), 11125−11143.
(35) Wang, S.; Xing, J.; Chatani, S.; Hao, J.; Klimont, Z.; Cofala, J.; Amann, M. Verification of anthropogenic emissions of China by satellite and ground observations. *Atmos. Environ.* **2011**, *45* (35), 6347−6358.
(36) Fu, X.; Zhang, H.; Wang, X.; Yu, B.; Lin, C.-J.; Feng, X. Observations of atmospheric mercury in China: a critical review. *Atmos. Chem. Phys. Discuss.* **2015**, *15* (8), 11925−11983.
(37) Fu, X.; Zhu, W.; Zhang, H.; Sommar, J.; Yu, B.; Yang, X.; Wang, X.; Lin, C.-J.; Feng, X. Depletion of atmospheric gaseous elemental mercury by plant uptake at Mt. Changbai, Northeast China. *Atmos. Chem. Phys.* **2016**, *16* (20), 12861−12873.
(38) Fu, X. W.; Feng, X. B.; Dong, Z. Q.; Yin, R. S.; Wang, J. X.; Yang, Z. R.; Zhang, H. Atmospheric gaseous elemental mercury (GEM) concentrations and mercury depositions at a high-altitude mountain peak in south China. *Atmos. Chem. Phys.* **2010**, *10* (5), 2425−2437.
(39) Fu, X. W.; Feng, X. B.; Liang, P.; Zhang, H.; Ji, J.; Liu, P. Temporal trend and sources of speciated atmospheric mercury at Waliguan GAW station, Northwestern China. *Atmos. Chem. Phys.* **2012**, *12* (4), 1951−1964.
(40) de Foy, B.; Tong, Y.; Yin, X.; Zhang, W.; Kang, S.; Zhang, Q.; Zhang, G.; Wang, X.; Schauer, J. J. First field-based atmospheric observation of the reduction of reactive mercury driven by sunlight. *Atmos. Environ.* **2016**, *134*, 27−39.
(41) Liu, M.; Chen, L.; Xie, D.; Sun, J.; He, Q.; Cai, L.; Gao, Z.; Zhang, Y. Monsoon-driven transport of atmospheric mercury to the South China Sea from the Chinese mainland and Southeast Asia—Observation of gaseous elemental mercury at a background station in South China. *Environ. Sci. Pollut. Res.* **2016**, *23* (21), 21631−21640.
(42) Fu, X.; Feng, X.; Zhu, W.; Zheng, W.; Wang, S.; Lu, J. Y. Total particulate and reactive gaseous mercury in ambient air on the eastern slope of the Mt. Gongga area, China. *Appl. Geochem.* **2008**, *23* (3), 408−418.
(43) Guo, Y.; Feng, X.; Li, Z.; He, T.; Yan, H.; Meng, B.; Zhang, J.; Qiu, G. Distribution and wet deposition fluxes of total and methyl mercury in Wujiang River Basin, Guizhou, China. *Atmos. Environ.* **2008**, *42* (30), 7096−7103.
(44) Wan, Q.; Feng, X.; Lu, J.; Zheng, W.; Song, X.; Li, P.; Han, S.; Xu, H. Atmospheric mercury in Changbai Mountain area, northeastern China II. The distribution of reactive gaseous mercury and particulate mercury and mercury deposition fluxes. *Environ. Res.* **2009**, *109* (6), 721−727.
(45) Fu, X.; Feng, X.; Zhu, W.; Rothenberg, S.; Yao, H.; Zhang, H. Elevated atmospheric deposition and dynamics of mercury in a remote upland forest of southwestern China. *Environ. Pollut.* **2010**, *158* (6), 2324−2333.
(46) Huang, J.; Kang, S.; Zhang, Q.; Yan, H.; Guo, J.; Jenkins, M. G.; Zhang, G.; Wang, K. Wet deposition of mercury at a remote site in the Tibetan Plateau: Concentrations, speciation, and fluxes. *Atmos. Environ.* **2012**, *62*, 540−550.
(47) Zhou, J.; Feng, X.; Liu, H.; Zhang, H.; Fu, X.; Bao, Z.; Wang, X.; Zhang, Y. Examination of total mercury inputs by precipitation

DOI: 10.1021/acs.est.9b02428
Environ. Sci. Technol. 2019, 53, 8938−8946

and litterfall in a remote upland forest of Southwestern China. *Atmos. Environ.* **2013**, *81*, 364−372.
(48) Fu, X.; Yang, X.; Lang, X.; Zhou, J.; Zhang, H.; Yu, B.; Yan, H.; Lin, C. J.; Feng, X. Atmospheric wet and litterfall mercury deposition at urban and rural sites in China. *Atmos. Chem. Phys.* **2016**, *16* (18), 11547−11562.
(49) Ministry of Ecology and Eenvirenment of the People's Republic of China (MEE). *Emission Standard of Air Pollutants for Thermal Power Plants (GB13223-2011)*; MEE: Beijing, China, 2011.
(50) Pai, P.; Karamchandani, P.; Seigneur, C.; Allan, M. A. Sensitivity of simulated atmospheric mercury concentrations and deposition to model input parameters. *J. Geophys. Res.* **1999**, *104* (D11), 13855−13868.
(51) Roustan, Y.; Bocquet, M. Sensitivity analysis for mercury over Europe. *J. Geophys. Res.* **2006**, *111* (D14), 1−16.
(52) Lin, C.-J.; Pongprueksa, P.; Bullock, O. R., Jr; Lindberg, S. E.; Pehkonen, S. O.; Jang, C.; Braverman, T.; Ho, T. C. Scientific uncertainties in atmospheric mercury models II: Sensitivity analysis in the CONUS domain. *Atmos. Environ.* **2007**, *41* (31), 6544−6560.
(53) Pudasainee, D.; Kim, J.-H.; Yoon, Y.-S.; Seo, Y.-C. Oxidation, reemission and mass distribution of mercury in bituminous coal-fired power plants with SCR, CS-ESP and wet FGD. *Fuel* **2012**, *93*, 312−318.
(54) Wang, F.; Wang, S.; Zhang, L.; Yang, H.; Wu, Q.; Hao, J. Mercury enrichment and its effects on atmospheric emissions in cement plants of China. *Atmos. Environ.* **2014**, *92*, 421−428.
(55) Lindberg, S. E.; Stratton, W. J. Atmospheric mercury speciation: Concentrations and behavior of reactive gaseous mercury in ambient air. *Environ. Sci. Technol.* **1998**, *32* (1), 49−57.
(56) Seigneur, C.; Vijayaraghavan, K.; Lohman, K.; Karamchandani, P.; Scott, C. Global Source Attribution for Mercury Deposition in the United States. *Environ. Sci. Technol.* **2004**, *38* (2), 555−569.
(57) United Nations Environment Programme (UNEP). *Global Mercury Assessment 2018: Sources, Emissions, Releases and Environmental Transport*; UNEP: Geneva, Switzerland, 2018.

DOI: 10.1021/acs.est.9b02428
Environ. Sci. Technol. 2019, 53, 8938−8946